EBioMedicine 52 (2020) 102618

Contents lists available at ScienceDirect

EBioMedicine

journal homepage: www.elsevier.com/locate/ebiom

Research paper

Sphere-induced reprogramming of RPE cells into dual-potential RPE stem-like cells

Fenghua Chen[a,d,1], Xiao Liu[a,e,1], Yao Chen[a,f,1], John Y. Liu[a], Huayi Lu[a,g], Wei Wang[a], Xiaoqin Lu[a], Kevin C. Dean[a], Ling Gao[e], Henry J. Kaplan[a], Douglas C. Dean[a,b,c,*], Xiaoyan Peng[d,**], Yongqing Liu[a,b,c,*]

[a] Department of Ophthalmology and Visual Sciences, University of Louisville School of Medicine, 301 E Muhammad Ali Blvd, Louisville, Kentucky 40202, USA
[b] James Graham Brown Cancer Center, University of Louisville School of Medicine, Louisville, Kentucky 40202, USA
[c] Birth Defects Center; University of Louisville School of Medicine, Louisville, Kentucky 40202, USA
[d] Department of Ophthalmology, Beijing Tongren Hospital, Capital Medical University, Beijing 100005, China
[e] Department of Ophthalmology, Second Affiliated Hospital of Xiangya Medical School, Central South University, Changsha, China
[f] Department of Ophthalmology, Xiangya Hospital, Central South University, Changsha, China
[g] Second Hospital of Jilin University, Changchun, Jilin Province, China

ARTICLE INFO

Article History:
Received 1 May 2019
Revised 20 November 2019
Accepted 18 December 2019
Available online xxx

Keywords:
RPE stem cells
Sphere-induced reprogramming
Retina degeneration
Cell transplantation

ABSTRACT

Background: The retinal pigment epithelium (RPE) has the potential to regenerate the entire neuroretina upon retinal injury in amphibians. In contrast, this regenerative capacity has been lost in mammals. The reprogramming of differentiated somatic cells into induced pluripotent stem cells (iPSCs) by viral transduction of exogenous stem cell factors has triggered a revolution in regenerative medicine. However, the risks of potential mutation(s) caused by random viral vector insertion in host genomes and tumor formation in recipients hamper its clinical application. One alternative is to immortalize adult stem cells with limited potential or to partially reprogram differentiated somatic cells into progenitor-like cells through non-integration protocols.

Methods: Sphere-induced RPE stem cells (iRPESCs) were generated from adult mouse RPE cells. Their stem cell functionality was studied in a mouse model of retinal degeneration. The molecular mechanism underlying the sphere-induced reprogramming was investigated using microarray and loss-of-function approaches.

Findings: We provide evidence that our sphere-induced reprogramming protocol can immortalize and transform mouse RPE cells into iRPESCs with dual potential to differentiate into cells that express either RPE or photoreceptor markers both *in vitro* and *in vivo*. When subretinally transplanted into mice with retinal degeneration, iRPESCs can integrate to the RPE and neuroretina, thereby delaying retinal degeneration in the model animals. Our molecular analyses indicate that the Hippo signaling pathway is important in iRPESC reprogramming.

Interpretation: The Hippo factor Yap1 is activated in the nuclei of cells at the borders of spheres. The factors Zeb1 and P300 downstream of the Hippo pathway are shown to bind to the promoters of the stemness genes *Oct4*, *Klf4* and *Sox2*, thereby likely transactivate them to reprogram RPE cells into iRPESCs.

Fund: National Natural Science Foundation of China and the National Institute of Health USA.

1. Introduction

The fertilized oocyte gives rise to all cells in the body through ontogenesis. Every single somatic cell has the same set of genetic material required for developing into a complete individual as is found in the zygote but exhibits a different capacity to realize this potential because of its specific epigenetic settings and lack of maternal factors that control genomic expression [1]. A small number of adult stem cells are retained in some adult human tissues and organs for cellular homeostasis such as limbus stem cells for the corneal

* Corresponding authors at: Department of Ophthalmology and Visual Sciences, University of Louisville School of Medicine, 301 E Muhammad Ali Blvd, Louisville, Kentucky 40202, USA.
** Corresponding author. Department of Ophthalmology, Beijing Tongren Hospital, Capital Medical University, Beijing, China.
E-mail addresses: dcdean01@louisville.edu (D.C. Dean), drpengxy@163.com (X. Peng), y0liu016@louisville.edu (Y. Liu).
[1] These authors contribute equally.

https://doi.org/10.1016/j.ebiom.2019.102618

Research in context

Evidence before this study

Age-related macular degeneration (AMD), a leading cause of blindness in seniors, is caused initially by dysfunction of the retinal pigment epithelium (RPE) and subsequently by loss of photoreceptors in the retina. Stem cell-based therapy to restore both the deteriorated RPE and neuroretina is thought to be one of the effective ways to treat the disease. Several mammalian stem cell sources, including retinal stem cell (RSC), Müller glial stem cell (MGSC), and RPE stem cell (RPESC), have been reported to be adult tissue-specific progenitors with a restricted renewal capacity and potential to differentiate into cells expressed markers of photoreceptors *in vitro*. However, none of these stem cells present the dual potential to differentiate into both RPE and photoreceptor cells, and they are not functional after transplanted into recipient eyes. Induced pluripotent stem cells (iPSCs) are generated by viral transduction of a number of exogenous stem cell factors to differentiated somatic cells and they can differentiate into either RPE or photoreceptor cells *in vitro.* These resultant tissue-specific cells can accordingly integrate into the RPE or the neuroretina in model animals to functionally rescue or slow their visual deterioration.

Added value of this study

Sphere-induced RPE stem cells (iRPESCs) with the dual-potential to become RPE and photoreceptor cells are generated by our non-virus integration reprogramming method and do not need be directed to differentiate into either RPE or photoreceptor cells *in vitro* before transplanted to recipient animals to functionally rescue the degenerated retinas of model mice.

Implications of all the available evidence

Mouse iRPESCs have the dual-potential to simultaneously replace lost RPE and photoreceptor cells in model mice of retinal degeneration. When successfully translated to human, they might be a suitable candidate for AMD treatment in the clinic.

epithelium [2]. The number of these cells and their capacity to replace lost cells and restore the function of compromised tissues decrease over time, often leading to age-related disorders [2]. Age-related macular degeneration (AMD) is one such disease. AMD is initially evidenced by the accumulation of drusen on the Bruch's membrane and the dystrophy of the retinal pigment epithelium (RPE), a single layer of epithelial cells between the neuroretina and the choroid, and subsequently by loss of photoreceptors in the retina that perceive light photons and transmit them as electric signals through other neurons to the brain to form visual images [3]. Unfortunately, no residential stem cells that can functionally replace the lost RPE and photoreceptor cells *in situ* have been identified to date; the search for a suitable stem cell source is therefore an ongoing effort for the treatment of AMD.

An ideal stem cell source for AMD treatment in a clinical trial is thought to exhibit two properties: it can expand towards a correct ontogenetic stage with limited potential *in vitro* and can functionally integrate into both the neuroretina and the RPE upon transplantation. Several mammalian stem cell sources, including retinal stem cells (RSC) [4], Müller glial stem cells (MGSC) [5], and RPE stem cells (RPESC) [6], have been reported to be adult tissue-specific progenitors with a restricted renewal capacity and potential to differentiate into cells expressed markers of photoreceptors *in vitro*. However, none of these stem cells present the dual potential to differentiate into both RPE and photoreceptor cells, and they are not functional after transplantation into recipient eyes [7]. Embryonic stem cells (ESCs) and induced pluripotent stem cells (iPSCs) can differentiate into either RPE or photoreceptor cells *in vitro* [8–10]. The resultant tissue-specific cells can integrate into the RPE or the neuroretina in model animals to functionally rescue or slow their visual deterioration [8–10]. However, there are two major challenges to using ESCs or iPSCs in the clinic. First, the undifferentiated cells within a heterogeneous population derived from the 'directed' differentiation of ESC/iPSCs are extremely tumorigenic *in vivo*. Second, it is difficult to differentiate the cells into more than one target cell type using a single differentiation protocol, making this approach inapplicable to the simultaneous replacement of multiple lineages damaged by diseases such as AMD in which both RPE and photoreceptor cells are affected. Both the neuroretina and the RPE are derivatives of the optic neuroepithelium, and it is logical to hypothesize that stem cells derived from either the RPE or neuroretinal cells would have the potential to differentiate into cells of both tissues. In amphibians, fully matured and mitotically quiescent RPE cells can be stimulated *in vivo* to proliferate and transform to a stem-like state upon traumatic damage to the eye, to repopulate the RPE and give rise to all lineages in the regenerated neuroretina [11]. In contrast, similar damage to the mammalian RPE and/or retina that would also cause RPE cell proliferation does not result in any ocular tissue regeneration but instead leads to a pathogenesis known as proliferative vitreoretinopathy (PVR) in humans. In other words, the mammalian RPE has lost the capacity to regenerate either itself or the neuroretina [12]. Despite this, we reason that mammalian RPE tissues retain their developmental signatures in their epigenetic genomes and that their dual potential to reproduce RPE cells and to transdifferentiate into retinal lineages when certain intrinsic and/or extrinsic factors are encountered. Based on our previous work [13], we developed and used a sphere-induced reprogramming protocol to generate induced RPE stem cells (iRPESCs) from adult mouse RPE cells in culture. Here, we show that these iRPESCs exhibit a dual potential to differentiate into both RPE- and photoreceptor-like cells *in vitro* and *in vivo* and that they integrate into both the RPE and neuroretina and significantly delay retinal degeneration in model mice.

2. Materials and methods

2.1. Animals and cell transplantation

For *in vivo* differentiation, a total of 2×10^5 iRPESCs in a volume of 2 μl were subretinally transplanted into one eye of four 3-month-old C57BL/6J mice in the temporal area close to the optical nerve through the limbus, the vitreous, and the retina using a 30-gauge needle after the animal was anesthetized by intraperitoneal (IP) injection of a mixture of 100 mg ketamine and 10 mg xylazine per kg of body weight. The same number of RPE cells were delivered into the other eye in the same way. To assess the functionality of the iRPESCs *in vivo,* a pharmaceutical mouse model of retinal degeneration was used as the recipient. Seven 3-month-old C57BL/6J mice received a single intravenous (IV) injection of 25 mg/kg sodium iodate ($NaIO_3$), which initially causes RPE damage and consequently affects the neuroretina, leading to complete vision loss in 2 weeks [14,15]. Five days after $NaIO_3$ injection, iRPESCs were subretinally transplanted. The other eye received 2 μl of PBS as a control. All aspects of this study were conducted in accordance with the policies and guidelines set forth by the Institutional Animal Care and Use Committee and were approved by the University of Louisville, Kentucky, USA.

2.2. Primary RPE cell isolation and iRPESC preparation

Two transgenic mouse strains tagged with either the *LacZ* gene in a mixed C57BL/6J and S129 background or the *BEST1* promoter-

driven *tdTomato* gene in the C57BL/6J background were used to isolate RPE cells. Approximately 8–10 eyeballs of each strain were enucleated from 25 to 30-day-old pups that had been euthanized with CO_2. Enucleated eyecups were surface-disinfected and dissected to carefully remove the anterior portion of eye tissues using a pair of tweezers, including the cornea, the iris, the lens and the ciliary body, reserve the posterior portion of eyecups. The retina was separated from the posterior portion of eyecups, and the rest ocular tissues were incubated in a 0.25% trypsin solution at 37°C for 5 min. The RPE sheets were scraped off the choroid using a glass rod into a culture dish coated with 0.1% gelatin and were then cultured under 5% CO_2 at 37°C in DMEM with 10% FBS and 1% penicillin/streptomycin antibiotics (Invitrogen). To generate iRPESCs, monolayer-cultured primary RPE cells were first passaged 2 times at a 1:1 ratio. At the third passage (P3), they were scraped off the plates, pipetted vigorously to break up cell sheets, and transferred to an ultra-low adherence dish to form spheres of 500–800 cells in DMEM for 3 days. These spheres were then placed onto a feeder layer of mouse SNL fibroblasts (a gift from Dr. Qingxiao Lu) that were irradiation-inactivated to prevent cell proliferation [16]. These cells were cultured in mouse ESC-conditioned medium (1:1 ESC-cultured medium versus fresh mouse ESC medium, i.e., DMEM with 15% FCS, 0.1 mM nonessential amino acids, 0.03 mM nucleosides, 100 units/ml leukemia inhibitory factor, 2 mM L-glutamine, 0.1 mM β-mercaptoethanol, and 1% penicillin/streptomycin antibiotics) under 5% CO_2 at 37°C in a hypoxia (3% O_2) chamber for 21 days.

2.3. Photoreceptor and RPE cell differentiation

For photoreceptor cell differentiation, three-day-old spheres of mouse RPE cells and iRPESCs were cultured in the mouse photoreceptor cell differentiation medium (DMEM/F12 with 1× nonessential amino acids, 1× sodium pyruvate, 1× B27, 1× N_2 supplements, 10 ng/ml mouse noggin, 10 ng/ml Dkk-1, 10 ng/ml IGF-1, 5 ng/ml bFGF, and 1× penicillin/streptomycin antibiotics) under 5% CO_2 at 37°C for 0, 7, 14, and 21 days. For RPE cell differentiation, 0-, 7-, 14-, and 21-day old spheres of mouse iRPESCs were adherently cultured in DMEM medium with 5% FBS under 5% CO_2 at 37°C for 3 days [17].

2.4. Tumor formation in athymic nude mice

A total of 2×10^5 iRPESCs were subcutaneously injected into the hind limbs of athymic nude mice (Jackson Laboratory, Stock #: 007850) to form tumors as previously described [18].

2.5. Visual optokinetic response (OKR) assessment

Mouse visual function was assessed using a noninvasive OptoMotry© optokinetic testing system (CerebralMechanics, www.cerebralmechanics.com). Briefly, a test mouse was placed unrestrained on a central platform after 30 min of dark adaptation; the platform was surrounded by 4 monitors displaying alternative vertical white and black stripes moving either clockwise or counterclockwise to test the right or left eye, respectively. Her reflexive head movement behavior was recorded. Testing was initiated by projecting a moving image of low spatial frequency (0.042 cycles/degree (c/d)), rotating at 12 degrees/second. The spatial frequency of the grating was increased until the animal no longer responded. The threshold of maximum spatial frequency that a mouse can track correlates with her visual acuity [19]. The assessment was repeated by two persons blinded to the treatment of animals.

2.6. Immunofluorescence (IF)

Cells/spheres were adherently cultured in 8-well chamber glass slides coated with 0.1% gelatin for 2 days or as otherwise specified. They were fixed with 4% paraformaldehyde, rinsed with PBS, and blocked with 1% BSA and 3% serum from the species in which the secondary antibody was raised. For immunostaining, the primary antibodies that were used are listed in supplementary Table S1. Nuclei were counterstained with Hoechst dye (1:500, Invitrogen cat. H1399), and images were captured with a Zeiss fluorescence microscope.

2.7. Immunohistochemistry (IHC)

Eyeballs from cell-transplanted and PBS-sham-treated control mice were frozen in optimal cutting temperature (OCT) medium for at least 4 hours. The frozen tissues were cryosectioned for immunohistochemistry with the primary antibodies listed in Supplementary Table S1.

2.8. Real-time quantitative PCR (qPCR)

Total RNA from RPE cells, RPE spheres, and iRPESCs was extracted using TRIzol solution (Invitrogen), and cDNA was synthesized using the Invitrogen RT kit (Invitrogen). SYBR Green (Molecular Probes) qPCR was performed using the Stratagene Mx3000P system [18]. PCR primer sets were designed using the website-based program Primer3; their sequences are listed in supplementary Table S2. The relative amounts of the target cDNA were estimated by the threshold cycle (Ct) values using the double delta method ($2^{-(\Delta Ct_1 - \Delta Ct_2)} = 2^{-\Delta\Delta Ct}$, where sample 1 is compared to sample 2) [20] and normalized to the levels of the housekeeping gene *Gapdh* or *Actb*. At least 3 biological samples were analyzed, each in duplicate.

2.9. Affymetrix microarray analyses

TRIzol extraction of total RNA (Invitrogen) followed by RNeasy column cleanup (Qiagen) was performed according to the manufacturers' instructions. Probes were prepared for hybridization to a mouse genome Affymetrix Mouse Gene 2.0 ST Array according to the manufacturer's instructions. The hybridization images were processed using Affymetrix GeneChip Command Console® software. The raw intensity data were log2-transformed and normalized across all the samples and all gene spots upon GC content background correction. A genomic expression heat map was assembled using two programs, 'Cluster' and 'TreeView', for relative comparisons between experimental samples [13]. The Ingenuity Pathway Analysis program (Qiagen) was used to predict the activation of signaling pathways based on the microarray data.

2.10. Lentiviral shRNA

The short hairpin RNA (shRNA) oligomer used for Yap1 silencing was 5'- GCCATGACTCAGGATGGA. The lentiviral vector construction and virus assembly procedures were as described previously [21]. Primary mouse RPE cells were infected in culture by Yap1 shRNA lentivirus. The transduction efficiency was >70% based on EGFP-positive cell counts.

2.11. Western blotting (WB)

After Yap1 shRNA (Yap1_sh) or EGFP vector control (Vector_ctrl) lentivirus infection, the transduced primary RPE cells were lysed in protein extraction lysis buffer on ice for 20 min, followed by a 10-min centrifugation at 13,000 rpm. The supernatant was then immediately collected as the nondenatured protein extract for WB analysis. A 4–21% gradient SDS-PAGE gel was loaded with 10 μg of the above crude protein lysate, and electrophoresis was performed at 120 V for 60 min. The proteins in the gel were transferred to a PVDC membrane at 4°C overnight. Yap1 and β-actin antibodies (supplementary Table S1) were then hybridized to the protein membrane.

2.12. Chromatin immunoprecipitation (ChIP) assay

ChIP assays were performed as previously described using formaldehyde to crosslink the genomic DNA of wild-type MEF cells [13,18,22]. The chromatin was sheared to an average length of 300−500 bp. Polyclonal antiserum for Zeb1 (a kind gift from Dr. Douglas Darling) was used for immunoprecipitation. Equal amounts of preimmune serum were used as a control. The sequences of the primers for the *Sox2, Klf4,* and *Myc* promoters and the expected size of the PCR products are shown in Supplementary Table S3.

2.13. Statistical analysis

Where applicable, data were analyzed by two-tail unpaired t-test. Values in the graphs are presented as means ± standard deviations. Three-star '***' indicates p-value ≤ 0.001, two-star '**' indicates p-value ≤ 0.01, whereas one-star '*' indicates p-value ≤ 0.05. For all studies, results were obtained from at least 3 independent experiments of three technical replicates, unless otherwise specified.

3. Results

3.1. Dedifferentiation and senescence of mouse primary RPE cells in adherent culture

Since the RPE can regenerate the neuroretina in amphibians [11,23], we sought to determine whether mammalian RPE cells also possess such potential to differentiate into cells expressing retinal markers. We isolated RPE cells from CMV-LacZ-expressing mouse pups (see Methods) and cultured them to expansion (Fig. 1(a)). The

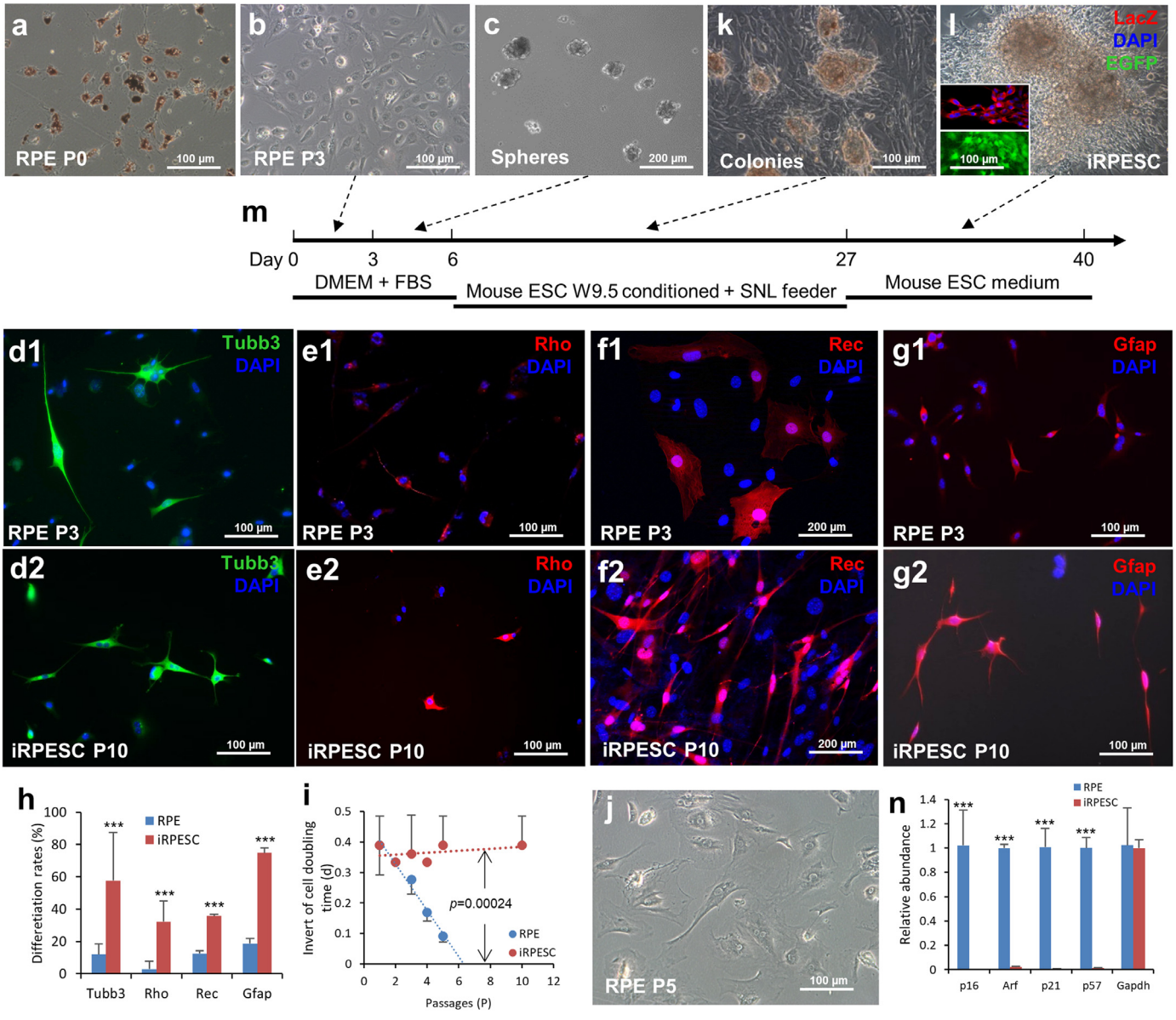

Fig. 1. Mouse RPE cell sphere-induced rejuvenation and reprogramming. (a) Mouse RPE cells at passage 0 (P0) isolated from RPE tissue. (b) Cultured RPE cells at P3. (c) P3 RPE cell spheres suspended in an ultra-low-adherence dish. (d) After 3 days of sphere formation, P3 RPE cells and iRPESCs were differentiated in mouse photoreceptor differentiation medium into cells expressing the general neural marker Tubb3, (e) the photoreceptor-specific markers rhodopsin (Rho) and (f) recoverin (Rec), and (g) the glial cell marker GFAP. (h) Bar graph comparing the differentiation rates of iRPESCs to RPE cells. (i) Graph comparing the cell proliferation rates of iRPESCs to RPE cells. (j) Representative image of monolayer-cultured senescent RPE cells at P5. (k) Colonies on feeder-layer cells. (l) iRPESCs were formed; their origin was confirmed by LacZ immunostaining (inset, red); and the cells were tagged by lentiviral EGFP (inset, green). (m) Diagram demonstrating the time course of the sphere-induced reprogramming process. (n) Bar graph comparing the expression of cyclin-dependent kinase inhibitor (CDKI) genes between RPE cells and iRPESCs. DMEM, Dulbecco's modified Eagle's medium; FBS, fetal bovine serum; ESC W9.5, embryonic stem cell line W9.5; ***$p < 0.001$.

monolayer cultures of mouse primary RPE cells initiated cell proliferation, followed by loss of pigment and transition to a fibroblastic morphology (Fig. 1(b)) [24]. The transition of postmitotic RPE cells to proliferative fibroblastic cells is known as the dedifferentiation process, through which they may regain some progenitor-like properties [12,25]. To test whether these dedifferentiated RPE cells possess certain stemness properties, we scraped off monolayer-cultured cells at passage 3 (P3), suspended the spheres in an ultra-low-adherence dish for 3 days (Fig. 1(c)), and then transferred them back to adherent culture in photoreceptor-differentiation medium [26]. After 21 days, a small number of these cells expressed the general neuron marker Tubb3, the rod-specific markers rhodopsin (Rho) and recoverin (Rec) (Fig. 1(d_1)–(f_1), and (h)). Some cells displayed the neuroglial marker Gfap (Fig. 1(g_1) and (h)), suggesting that mouse RPE cells have the potential to transdifferentiate into cells expressing neural and neuroglial markers *in vitro*. However, the proliferation rates of the mouse RPE cells quickly slowed down in culture (Fig. 1(i)), and the cells exhibited a stress-induced premature senescence (SIPS) [27] phenotype after 5 passages, with a larger and flatter cell morphology (Fig. 1(j)).

3.2. Sphere suspension culture rejuvenates RPE cells

To overcome this SIPS, we developed a rejuvenation protocol for mammalian cells *in vitro* [13,28]. Using this protocol, we generated spheres of mouse RPE cells (P3) and placed them in suspension culture for 3 days. Thereafter, we transferred them onto a feeder layer fibroblast cell line [16] and continued their adherent culture under hypoxia (3% O_2) in mouse ESC culture-conditioned medium (Fig. 1(k) and (m)). After 3 weeks, most of the mouse RPE sphere-derived cells died. However, a few survived and proliferated (Fig. 1(l)–(m)). Compared to their parent RPE cells, the sphere-derived cells were smaller and displayed a higher proliferative capacity with no sign of senescence for at least 10 passages (Fig. 1(i) and (l)), suggesting that they had been rejuvenated. These cells expressed significantly lower levels of cyclin-dependent kinase inhibitors (CDKIs), including *p16, Arf, p21*, and *p57*, than their parental RPE cells (Fig. 1(n)), indicating that constant repression of CDKI genes was the mechanism underlying their high proliferation capacity [29]. These sphere-derived RPE cells still expressed *LacZ*, confirming their RPE origin (Fig. 1(l) insert). To facilitate the tracking of these sphere-derived cells in transplanted animals, we further tagged them with EGFP expression by EGFP-lentivirus infection (Fig. 1(l) inset) [13].

3.3. Sphere-induced reprogramming of RPE cells into RPE stem-like cells

Self-renewal is an important characteristic of stem cells, and rejuvenation causes these RPE sphere-derived cells to undergo self-renewal [6] but not to become tumorigenic, as no tumors were detected after subcutaneous implantation into the nude mice (2 mice receiving 4 subcutaneous hind limb injections of 2×10^5 cells). Another characteristic of a stem-like phenotype is the expression of stem cell markers. These sphere-derived RPE cells expressed increased levels of *c-Myc*, which is a transcription factor required for the reprogramming of fibroblasts to iPSCs [30] and is likely a major regulator of self-renewal, as it is an oncogenic factor that maintains tumor cell proliferation [31]. Other adult stem cell markers such as *c-Kit, Cd44,* and *Abcg2* were significantly increased in the sphere-derived cells (Fig. 2(a)) [32], indicating that they resembled adult stem cells. Although no *Oct4* was detected by qPCR in the

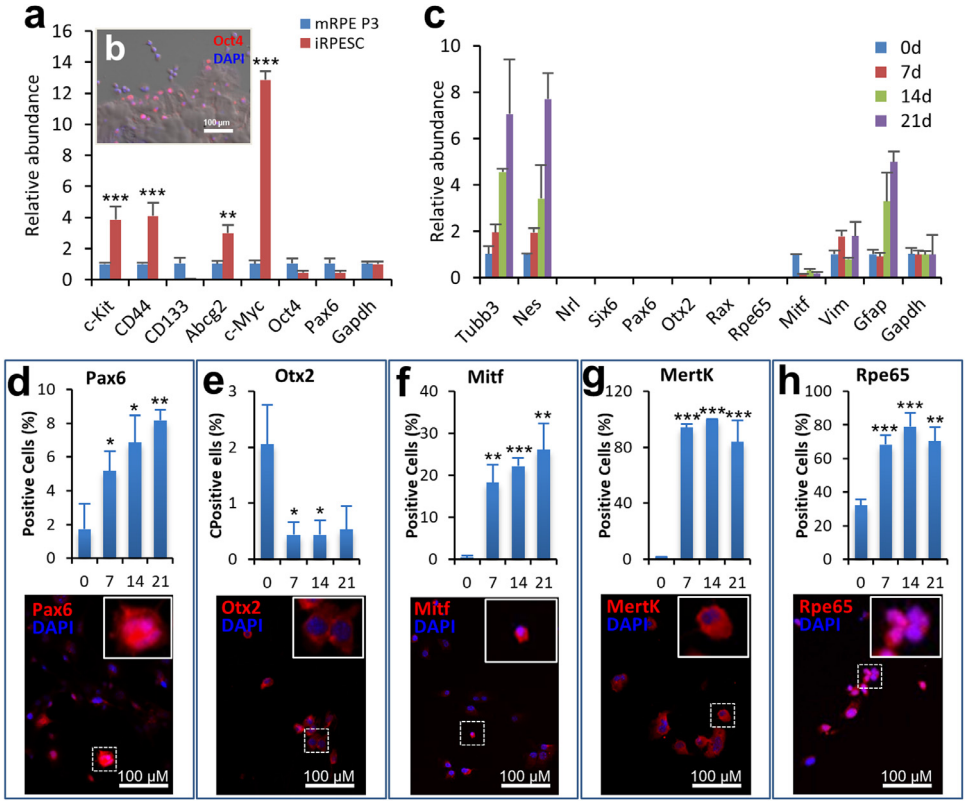

Fig. 2. Differentiation of iRPESCs *in vitro*. (a) Compared to their parental RPE cells, iRPESCs expressed higher levels of stem cell markers as detected by qPCR. (b) Transient expression of the stem cell marker Oct4 in sphere-derived RPE cells migrating out of a sphere. (c) Expression of marker genes detected by qPCR in iRPESCs after cultured in a photoreceptor cell differentiation medium for up to 21 days. (d) After subjecting to a RPE differentiation culture [17] for 0, 7, 14, and 21 days, the percentage of positive cells and a representative image of the 21-day differentiated cells with nuclear and cytoplasmic expression of the progenitor marker Pax6, (e) the nuclear expression of the progenitor mark Otx2, (f) the nuclear expression of the RPE differentiation regulator Mitf, (g) the surface expression of the RPE cell-specific marker Mertk, and (h) the cytoplasmic expression of the RPE cell-specific marker Rpe65. In panels d – h, the comparison is made between the control (0d) and other time points; $^{***}p < 0.001$; $^{**}p < 0.01$; $^{*}p < 0.05$.

sphere-derived cells, it was transiently detected by immunostaining in cells at the border of the spheres (Fig. 2(b)), suggesting that transient expression of this pluripotent stem cell gene might be critical for sphere-induced reprogramming [30]. Next, we checked whether the sphere-derived cells presented the potential to redifferentiate into retinal neurons and/or RPE cells *in vitro*. Using a mouse photoreceptor differentiation protocol [26], we were able to differentiate these RPE sphere-derived cells into cells expressing not only the neural markers Tubb3, Rho, Rec, and the neuroglial marker Gfap (Fig. 1 (d_2)–(g_2)) though none of them was PKC alpha positive (a marker for ON-bipolar cells) or the horizontal cell marker calbindin positive (data not shown). The expression of two general neural marker beta 3 tubulin (*Tubb3*) and nestin (*Nes*) and the neuroglial marker *Gfap* was gradually increased whereas that of early photoreceptor differentiation regulators such as *Six6, Pax6, Otx2, Rax,* and *Nrl* was hardly detected by qPCR throughout the photoreceptor differentiation (Fig. 2(c)). We previously found that sphere formation of dedifferentiated mouse RPE cells could redifferentiate them back to a differentiated phenotype [17]. Using such a protocol we re-made spheres of the sphere-derived cells for up to 21 days in suspension and then put them back to an adherent monolayer culture for 3 days. Immunostaining of these re-sphere-derived cells demonstrated that the RPE cell differentiation regulator Mitf was increasingly expressed in differentiating cells in accordance with the expression of the RPE cell markers Mertk and Rpe65 though only a few of Otx2 and Pax6 positive cells were detected in the nucleus (Fig. 2(d)–(h)). Taken together, the above evidence indicates that the sphere-derived cells possess dual potential, similar to RPE stem cells [11], not to retinal stem cells [25]. To determine whether primary RPE cells and RPE stem-like cells have the potential to differentiate *in vivo*, we subretinally transplanted either tdTomato-tagged RPE cells or EGFP-tagged RPE stem-like cells into C57BL/6J mice (see Methods). Three weeks later, cryosection immunostaining showed that no live transplanted RPE cells were apparent in the recipient eyes, though a small amount of tdTomato$^+$ cell debris was identified on the recipient RPE (Fig. 3 (a)). In contrast, the RPE stem-like cells were able to differentiate into both Rho$^+$ photoreceptor-like cells in the outer nuclear layer (ONL) (Fig. 3(b)) and RPE65$^+$ RPE-like cells in RPE tissue (Fig. 3(c)). Based on these observations, we conclude that these sphere-derived stem-like cells exhibit two major RPE stem cell features, i.e., self-renewal and

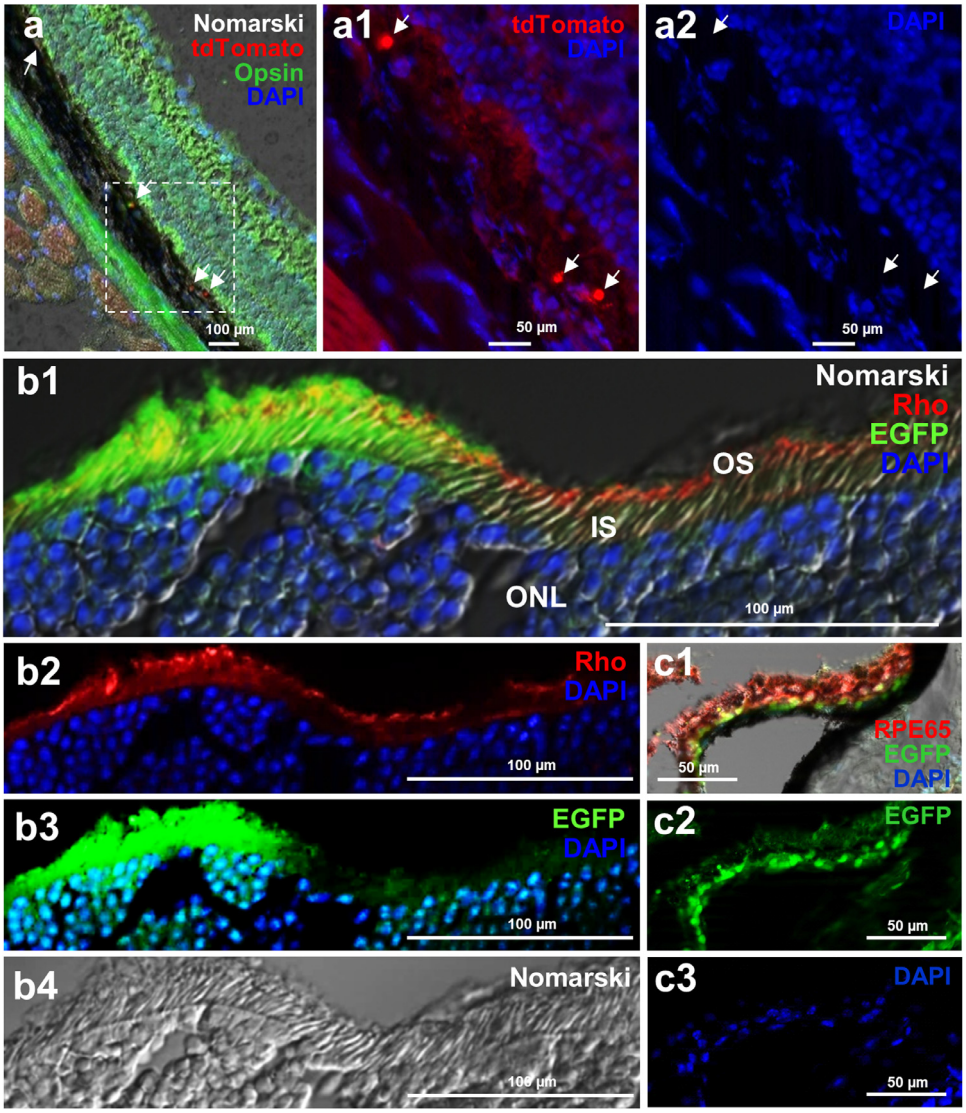

Fig. 3. Differentiation of iRPESCs *in vivo*. (a) After subretinal transplantation, fewer tdTomato-expressing RPE cells were only detected in the RPE tissue (white arrows), whereas (b) EGFP-expressing iRPESCs could differentiate into cells expressing the photoreceptor-specific marker Rho and (c) the RPE cell-specific marker RPE65. OS, outer segment; IS, inner segment; ONL, outer nuclear layer.

dual-potential to differentiate into both RPE and photoreceptor cells; therefore, we refer to these cells as sphere-induced RPE stem cells or iRPESCs.

3.4. *Survival of grafted iRPESCs* in vivo

Next, we investigated iRPESC survival in the grafted eyes. Compared to the primary RPE cells, which showed little survival in the grafted sites (Fig. 3(a)), we noted that the transplanted iRPESCs were mostly concentrated at the injection sites as small aggregates, although some of them had dispersed some distance as pairs or triplets or even as single cells at 3 weeks after transplantation (Fig. 4(a) and (b)). We reason that iRPESCs aggregated to survive the stressful subretinal environment, where lacking cell-cell or cell-matrix contact results in cell death (anoikis). Most of the transplanted iRPESCs, if not all, disappeared within 7 weeks (data not shown). We suspect that the grafted RPE cells died earlier of anoikis, whereas iRPESCs died later, likely due to host immune rejection, as we did not use immunodeficient mice as recipients and subretinal injection would overcome the retinal and subretinal immune privilege barrier [33,34].

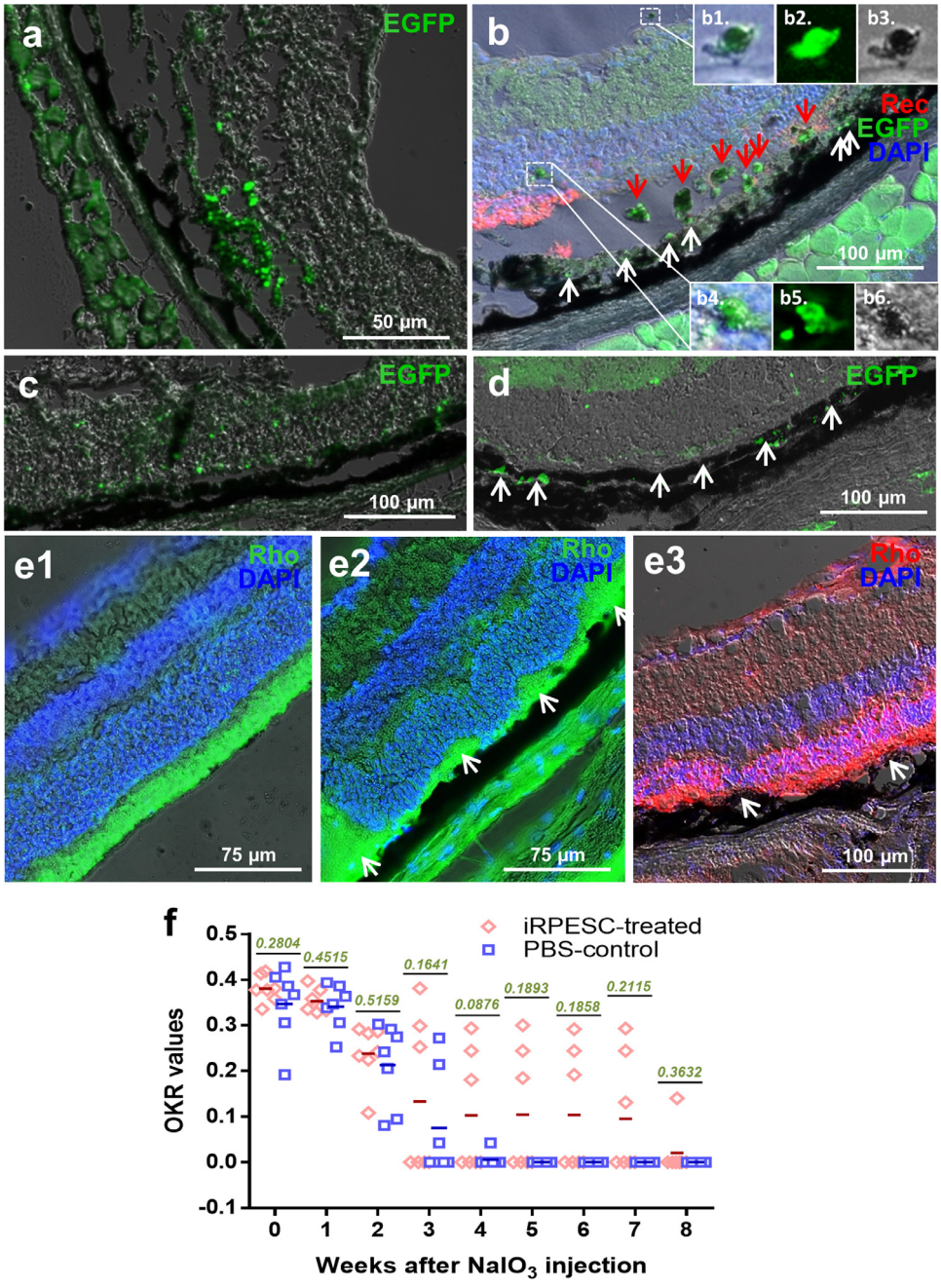

Fig. 4. Migration, integration, and functionality of iRPESCs in mice with retinal degeneration. (a) Most iRPESCs showing EGFP expression remained at the injection site. (b) Some of these cells aggregated in the subretinal space (red arrows), while some of them migrated through the retina (insets B_{4-6}) and even reached the vitreous (insets B_{1-3}) and integrated into the RPE (white arrows). (c) iRPESCs penetrated the retina and (d) integrated into the RPE (white arrows). (e) A pharmaceutical mouse model of retinal degeneration in which photoreceptor cells are affected following damage to the RPE and the ONL (white arrows) by sodium iodate ($NaIO_3$), a chemical that specifically targets RPE tissue, administered at a low dosage by intravenous (IV) injection. A representative retinal image of C57BL/6J mice (e1) before and (e2) 5 days after $NaIO_3$ administration, and (e3) 2 weeks after the transplantation of iRPESCs. (f) A visual optokinetic response (OKR) of the aforementioned mice was used to assess the functionality of the subretinally transplanted iRPESCs. *P* values of Student's *t*-tests are indicated for each time point comparison between PBS control and iRPESC-transplanted mice.

3.5. Migration and integration of transplanted iRPESCs in vivo

In the subretinal space of C57BL/6J mice, the transplanted iRPESCs could disperse a short distance (Fig. 4(a)). We observed that some of them migrated into the neuroretina (Fig. 4(b_{5-6}) and (c)), while some of them even passed through the retina and reached the vitreous (Fig. 4(b_{1-3})). In all 4 iRPESC-transplanted mice, the grafted iRPESCs were able to integrate into the RPE and to re-synthesize the pigment (Fig. 3(a) and (c), Fig. 4(b) white arrows), suggesting that they are ready to transdifferentiate by default back to their original RPE phenotype. In 1 out of 4 iRPESC-transplanted mice, we also detected EGFP and Rho double-positive regions along the ONL (Fig. 3(b)), indicating possible integration or fusion of iRPESCs with local photoreceptor cells [35,36]. The transplanted iRPESCs also integrated into the RPE tissue and expressed EGFP in all transplanted mice (Figs. 3(c), 4 (b), (d)).

3.6. Functionality of iRPESC in recipient retinas

As iRPESCs could integrate into both RPE and retinal tissues (Fig. 3 (b)–(c)), we wondered whether the transplanted iRPESCs could recover the reduction of vision caused by RPE damage-related photoreceptor degeneration, as observed in AMD patients. We adopted a pharmaceutical model of retinal degeneration in which photoreceptor cells were affected following specific damage to the RPE by intravenous injection of sodium iodate ($NaIO_3$) (Fig. 4(e)) [14,15]. Seven 3-month-old C57BL/6J mice were used for the experiment. Five days after the administration of 15 mg/kg $NaIO_3$, a total of 2×10^5 iRPESC cells in 2 μl of PBS was subretinally transplanted into one eye of the $NaIO_3$-treated mice, while the same amount of PBS was delivered similarly to the other eye as a negative control. The photopic response of both eyes was assessed by an optokinetic response (OKR) system every week until no visual response was detected. After $NaIO_3$ administration, the vision of the animals started to decline within 2 weeks in the PBS-sham-treated control eyes and 3 weeks in the iRPESC-transplanted eyes (Fig. 4(f)). At 4 weeks, all the PBS control eyes had completely lost their OKR response, while 3 of 7 the iRPESC-transplanted eyes still exhibited stabilized vision for 7 weeks (Fig. 4(f)). This result suggests that subretinal transplantation of iRPESCs could temporally maintain the vision of the affected mice.

To ensure that the above transplantation result was reproducible, we repeated the experiment with cells isolated from 3-week-old mouse RPE tissues whose origin had been tagged by BEST1-tdTomato expression (see Methods) (Fig. 5(a)). These BEST1-tagged RPE cells (BEST1-RPE) could be tracked even after they were reprogrammed into BEST1-tagged iRPESCs (BEST1-iRPESCs) (Fig. 5(b)) and redifferentiated into cells expressing Tubb3 and Opsin *in vitro* (Fig. 5(c)–(e)). One month after transplantation, many of the BEST1-iRPESCs regained pigmentation when they remained in a clump in the subretinal space (Fig. 5(f_{1-2})). As demonstrated in Figs. 3 and 4, a few of the transplanted BEST1-iRPESCs integrated into the outer nuclear layer (ONL) and became Rho^+ (Fig. 5(f_{3-6})) or integrated into the RPE (Fig. 5 (g)). These results confirm that BEST1-iRPESCs also present dual potential to differentiate into both retinal and RPE tissues *in vivo*.

3.7. Epigenetic modifications and iRPESC reprogramming

Cell-cell only contacts in suspended spheres resemble those in early embryos, in which cellular epigenetic codes may be reconfigured back to a more immature state [37]. To determine why adult

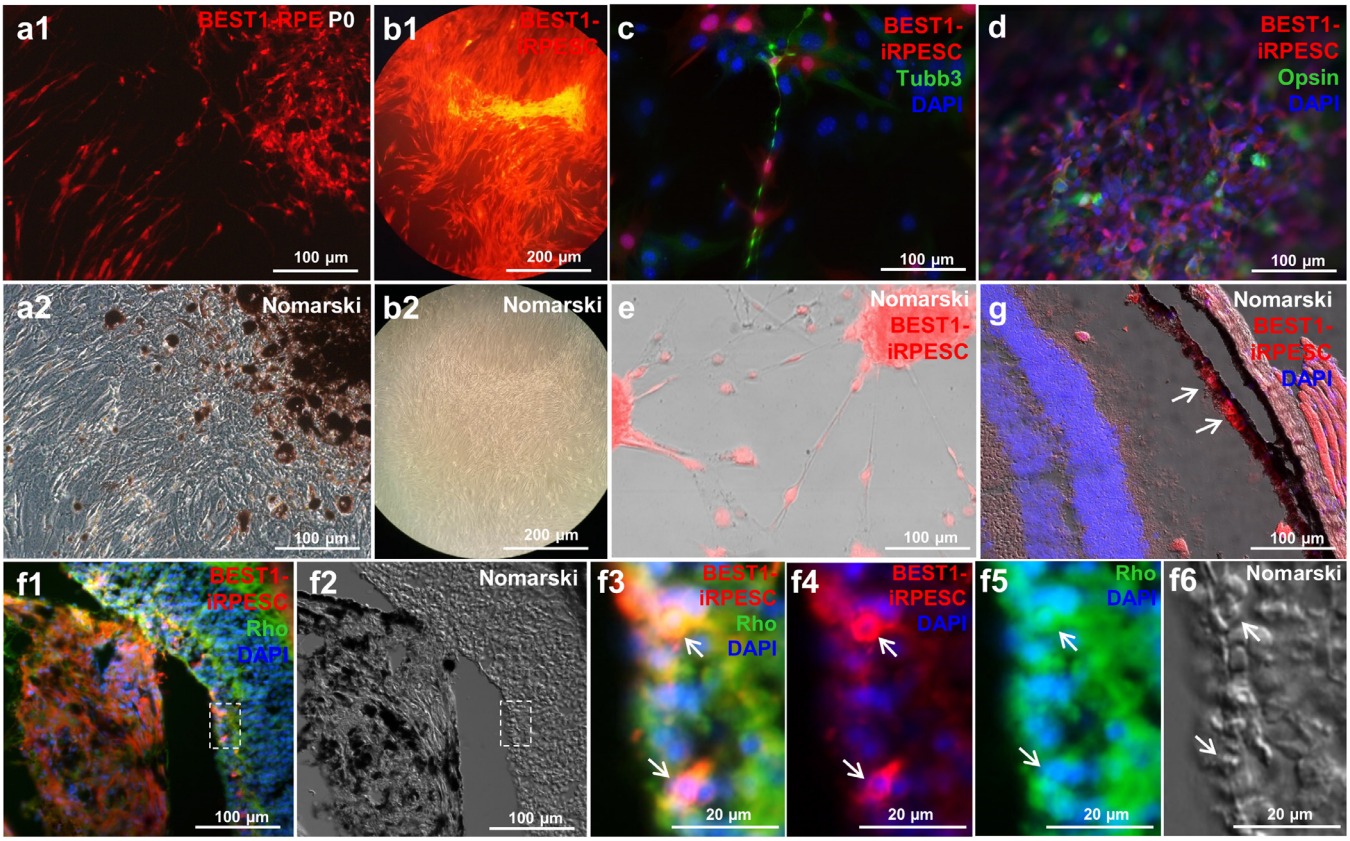

Fig. 5. RPE origin of iRPESCs tagged by BEST1-cre. (a) Cultured RPE cells were isolated from BEST1-cre mice in which the RPE was specifically tagged by expressing red fluorescent tdTomato. (b) BEST1-iRPESCs were produced from BEST1-RPE cell spheres. (c) BEST1-iRPESCs differentiated into cells expressing the general neural marker Tubb3 and (d) the photoreceptor-specific marker opsin *in vitro*. (e) BEST1-iRPESC spheres generated cells with a neuron-like morphology. (f) After being subretinally transplanted into recipient C57BL/6J mice, iRPESCs were integrated not only into the neuroretina (white arrows) but also (g) into the RPE (white arrows).

RPE cells could be reprogrammed into iRPESCs by sphere suspension culture, we conducted a genomic expression profiling experiment to compare iRPESCs or RPE spheres (RPE-SPs) to their parental RPE cells. The overall genomic expression heat map indicated that the expression profile of the iRPESCs was very different from that of their parental RPE; the change in genomic expression occurred immediately upon sphere formation, as the profiles of RPE-SPs and iRPESCs resembled each other (Fig. 6(a)). To elucidate the potential molecular mechanism underlying sphere-induced reprogramming, we focused on the expression of stem cell genes. Eight out of 15 selected genes, including *Klf4, Alpl, Kit, Kitl,* and *Bmi1* in RPE-SPs and *Abcg2, Bmi1, Cd44, Kitl,* and *c-Myc* in iRPESCs, were expressed at higher levels in RPE-SPs and/or iRPESCs compared with RPE (Fig. 6(b)), which was confirmed by qPCR (Fig. 2(a)). Next, we examined whether the expression of epigenetic modifier genes was upregulated in RPE-SPs and/or iRPESCs compared to RPE. Seven out of 15 selected genes, including two DNA methylation genes, *Dnmt1* and *Dnmt3a*, four histone acetylation genes, *Hat1, P300, Myst2*, and *Myst3*, and seven deacetylation genes, *Sirt2, Sirt6, Hdac1, Hdac2, Hdac3, Hdac5*, and *Hdac6*, were upregulated (Fig. 6(c)), which might facilitate the expression of master stemness genes such as *Oct4* and *Klf4* in RPE-SPs (Figs. 2(b) and 6(b)), resulting in the generation of iRPESCs.

3.8. Signaling pathways in iRPESC reprogramming

To identify which signaling pathways were activated during the reprogramming of RPE into iRPESCs, we adopted the Ingenuity Pathway Analysis program to obtain clues. We found that many growth factors, such as *Vegf, Tgf, Pdgf, Egf,* and *Ngf*, and their receptors, such as *Vegfr, Egfr, Pdgfr,* and *Tlk4*, as well as two stem cell-related signaling ligands, *Kitl* and *Lif,* were highly expressed in RPE-SPs and/or iRPESCs (Fig. 6(d)). This suggests a cascade of MAP kinase phosphorylation leading to cell proliferation (self-renewal) (Fig. 6(d)). These changes would also potentially activate biochemical reactions allowing cells to survive reprogramming-induced cellular stresses [38] that often result in cell death via both the Akt-mTor and Mitf-Bcl2 signaling pathways [39], where Mitf would upregulate *Dct, Tyr* and *Tyrp1* to synthesize pigment for RPE cell differentiation [40] (Fig. 6(d)). Interestingly, protein kinase C (*Pkc*), a master regulator of cell migration, was also upregulated in iRPESCs (Fig. 6(d)), which explains why the transplanted iRPESCs could migrate through the retina (Fig. 4(b)–(c)).

3.9. Wnt and Hippo signaling pathways are critical in sphere-induced reprogramming

Based on the above model, the cells at the border of the spheres had no neighboring cells on one side; therefore, the cell-cell

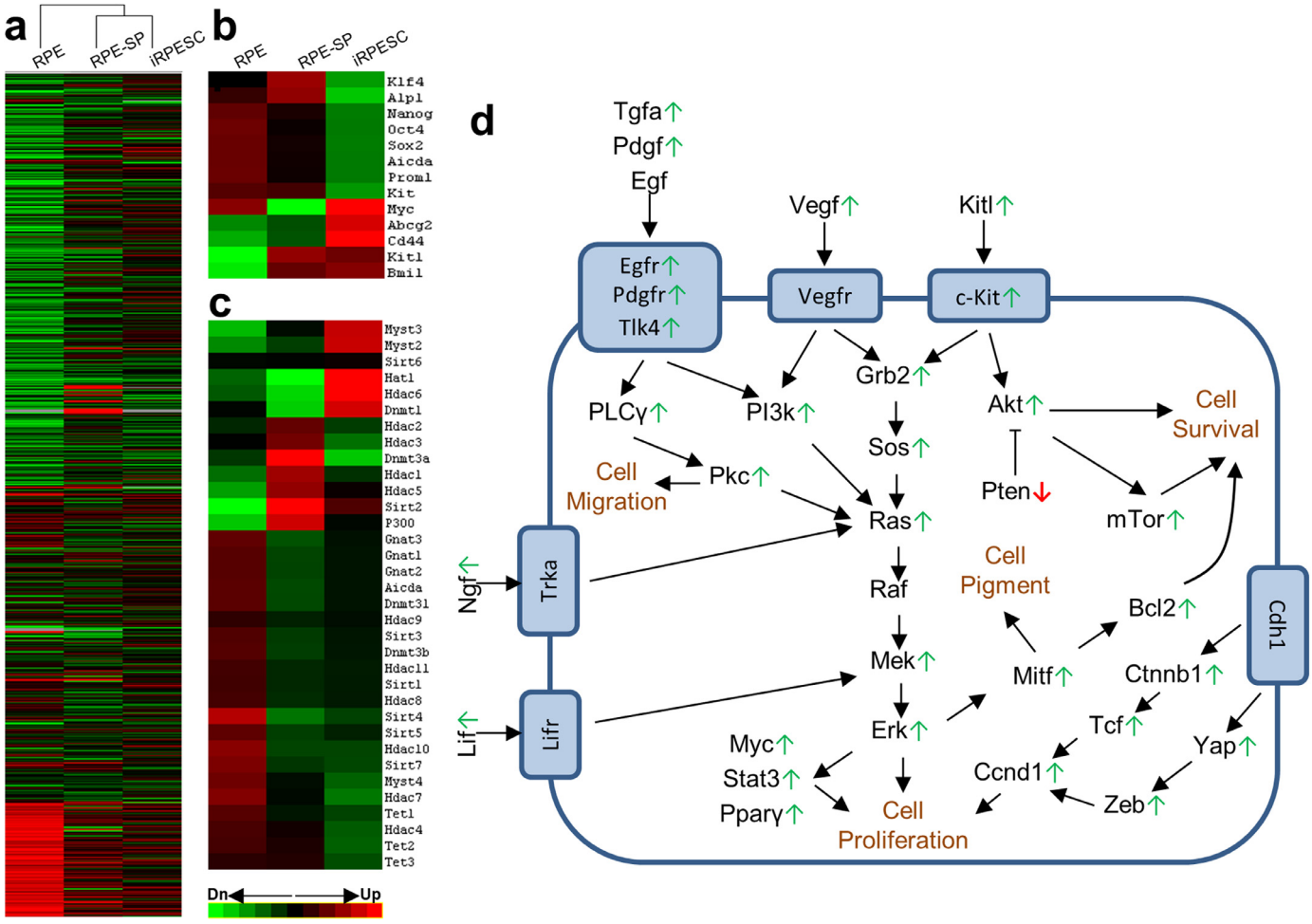

Fig. 6. Analysis of genomic expression in mouse RPE cells (RPE), RPE cell spheres (RPE-SP) and iRPESC to identify genes and pathways underlying sphere-induced reprogramming. (a) Affymetrix microarray genomic expression profiles of RPE, RPE-SP-, and iRPESC-indicate that sphere formation could modify cell genomic expression required for lineage reprogramming. (b) Expression of stemness genes. (c) Expression of epigenetic modifier genes. (d) Signaling pathways anticipated by the Ingenuity Pathway Analysis program as underlying potential mechanisms for reprogramming mouse RPE cells into iRPESCs. Green arrows indicate upregulation, while red arrows indicate downregulation.

adherence protein E-cadherin (Cdh1)-anchored β-catenin (Ctnnb1) might have been released from the membrane. Unanchored Ctnnb1 would enter the nuclei, wherein it would interact with Tcf/Lef transcription factors to transactivate the expression of cell cycle genes such as cyclin D1 (*Ccnd1*) to increase the cell proliferation rate (Fig. 6(d)) [41]. Our microarray data show that genes involved in the canonical Wnt/β-catenin pathway such as *Wnt5a, Fzd1, Ctnnb1, Tcf4*, and *Cnnd1* were upregulated in either RPE-SPs and/or iRPESCs compared to their parental RPE (Fig. 7(a)). The high expression of Ctnnb1 in RPE-SPs (Fig. 7(b)) in particular suggests that the canonical Wnt signaling pathway is important in the generation of iRPESCs, as reported in ESCs [41].

The Hippo pathway can be initiated when cells detach from each other and the Hippo factors Taz/Yap1 are activated in the nucleus [42], which will subsequently activate Zeb1 for cell proliferation [43,44]. As expected, our microarray data and immunostaining results showed that the Hippo factor Yap1 was not only upregulated but also activated in the nuclei of both RPE-SPs and iRPESCs (Fig. 7(c) and (d)). According to the current understanding of the Hippo pathway, Yap1/Taz are activated through guanine nucleotide-binding protein subunit alpha (Gna)11/12/13-coupled receptors (GPCRs) such as Fzd1 and Fak receptor tyrosine kinases (RTKs) such as Met when bound by their ligands, such as Wnt3a, Wnt5a/b, and growth factors such as Tgfb and Hgf [45]. Indeed, all of these genes were upregulated in RPE-SPs and/or iRPESCs (Fig. 7(a) and (d)), suggesting that Yap1-activated gene expression plays a critical role in sphere-induced reprogramming. As reported previously, Taz/Yap1 can bind and activate *Zeb1* expression [44], while Zeb1 together with its coactivator P300 binds and transactivates stemness genes such *Oct4* [13]; we also found that *Zeb1* and *P300* were upregulated in RPE-SPs (Fig. 7(d)) and that Zeb1 co-localized with nuclear Yap1 at the border of the spheres (Fig. 7(c) and (e)).

Since Sox2, Klf4 and Myc, in addition to Oct4, are essential factors in the generation of induced pluripotent stem cells (iPSCs) [30] and both *Klf4* and *Myc* were highly expressed in RPE-SPs or iRPESCs (Fig. 6(b)), we wondered whether Zeb1 binds their promoters, thereby potentially transactivating them. The hypothetical promoter sequences of *Sox2, Klf4*, and *c-Myc* all contain two potential Zeb1 binding sites (CANNTG) (Supplementary Fig. S1). Our chromatin immunoprecipitation (ChIP) assay showed that Zeb1 bound to the promoters of both *Sox2* and *Klf4* but not to that of *Myc* (Fig. 7(f)). To functionally test whether Yap1 affects the reprogramming of RPE cells into iRPESCs, we constructed, assembled, and used a lentivirus carrying Yap1 short hairpin RNA (Yap1_sh) to infect mouse RPE cells for the generation of iRPESCs. More than 70% of RPE cells were transduced by Yap1_sh, and the knockdown of Yap1 in these cells was confirmed by both qPCR and Western blotting (WB) (Fig. 7(g)–(h)). Knockdown of Yap1 decreased the proliferation of RPE cells (Fig. 7(i)) and their capacity to reprogram to iRPESCs (data not shown), suggesting an essential role of Yap1 in sphere-induced mouse RPE cell reprogramming.

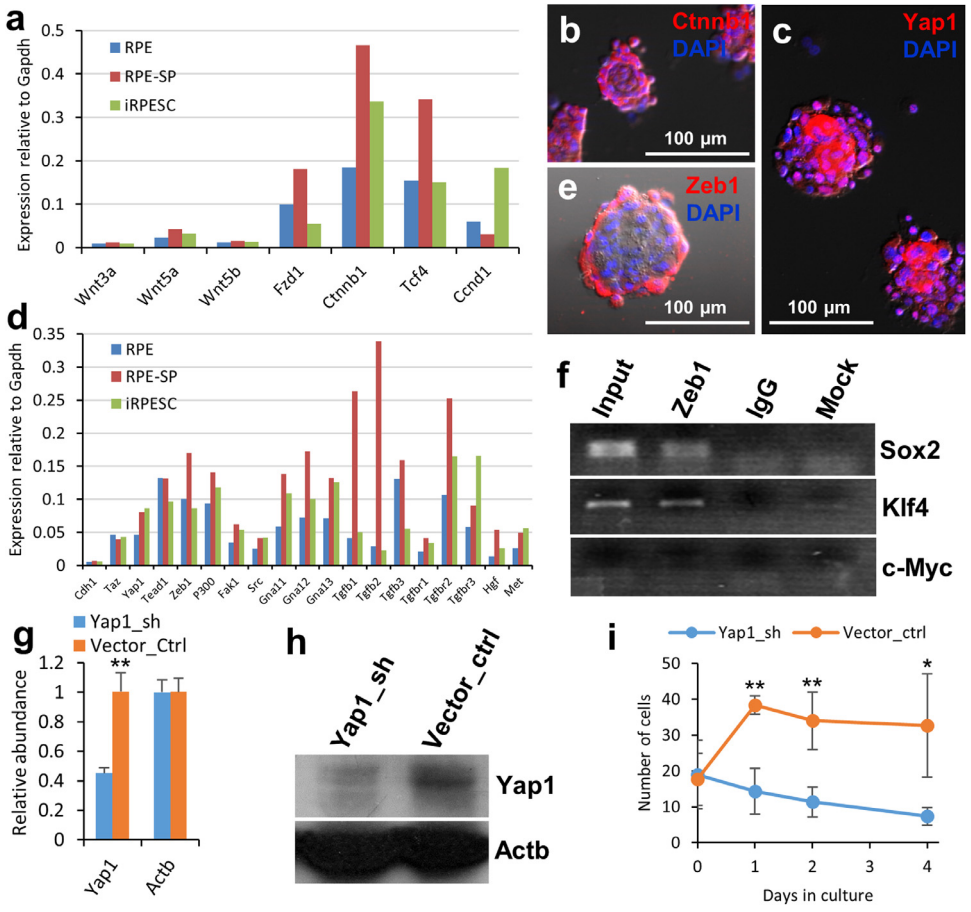

Fig. 7. Wnt and Hippo pathways involved in sphere-induced cell reprogramming. (a) Microarray data indicated that the Wnt pathway was activated in the RPE cell spheres, which was supported by the (b) sphere-induced accumulation of Ctnnb1. (c) The Hippo factor Yap1 was activated in the nuclei of the cells migrating out of the spheres and at the borders of the spheres. (d) Upregulation of elements involved in the Hippo pathway, including potential ligands, receptors, the co-factor Yap1, and downstream factors such as Zeb1 and P300 in the spheres. (e) Hippo-regulated Zeb1 accumulated in the cells at the borders of spheres. (f) Zeb1 was shown by chromatin immunoprecipitation (ChIP) to bind to stemness genes including *Klf4* and *Sox2*, in addition to *Oct4*. [13] Knockdown of the Hippo factor Yap1 (Yap1_sh) in RPE cells was validated by both (g) qPCR and (h) Western blotting (WB). (i) Knockdown of Yap1 inhibited cell proliferation compared to the vector control (Vector-ctrl).

4. Discussion

4.1. Sphere-induced cell rejuvenation

Spontaneous immortalization of murine fibroblasts is frequently observed after >20 passages in culture and is ascribed to silencing of p53 [46]. We did not detect any spontaneous immortalization of mouse RPE cells, as our mouse primary RPE culture never exceeded 5 passages. However, the senescent mouse RPE cells could be rejuvenated after 2–3 days of sphere reconditioning, a phenomenon reported previously in swine and human Müller glial cells (MGCs) [28]. The exact environmental factors required for sphere-induced cell rejuvenation are not known, though we hypothesize that depletion of nutrients, growth-stimulating factors, oxygen, and other damaging substances in suspended spheres would recondition the environment to allow cells to gradually adapt and thrive *in vitro*. It is therefore intriguing to test the hypothesis of whether the reduction of nutrients and oxygen in culture would prevent SIPS of primary murine RPE cells.

4.2. Efficiency of sphere-induced reprogramming

As it was difficult to obtain enough mouse primary RPE cells for our experiment, we initially used a large number of mouse eyecups to isolate RPE sheets (see Methods). After the first 2−3 passages, we could obtain approximately 5×10^5 cells and generate approximately 150 spheres of 500–800 cells in 3 days; thus, >80% of cells died at the end of the sphere culture. After being placed on a feeder layer and cultured under hypoxia (3% O_2) for 3 weeks, fewer than 10 colonies survived and expanded. Based on this result, only 0.003−0.013% of the murine RPE cells were reprogrammed to iRPESCs.

4.3. Dual potential of RPE cells and iRPESCs

Dedifferentiation occurred immediately when the isolated RPE cells were cultured in DMEM with FBS as the cells transitioned to manifest a fibroblast-like phenotype and depigmentation [25,44]. These dedifferentiated fibroblast-like cells readily redifferentiated into RPE-like cells after the formation of spheres *in vitro* [44] and into neuron progenitor-like cells (Fig. 1(d)). Based on this *in vitro* assessment, the dedifferentiated RPE cells appeared to possess a dual-potential RPE stem cell phenotype, similar to iRPESCs. However, compared to iRPESCs, RPE cells exhibited a limited proliferation capacity, and they senesced after 5 passages, whereas iRPESCs continued to proliferate through 10 passages (Fig. 1(i)). In addition, the primary RPE cells exhibited a limited differentiation potential compared to iRPESCs (Fig. 1(d)–(g)). This restriction of both the proliferation and differentiation capacities of RPE cells was even more obvious *in vivo* 3 weeks after subretinal transplantation. The grafted RPE cells became apoptotic in the recipient eyes and were not observed in the nearby retina, though some were apparently present in the RPE tissue (Fig. 3(a)). In contrast, iRPESCs demonstrated a capacity to penetrate (Fig. 4(b)–(c)) and possibly integrate into the retina (Figs. 3(b) and 5(f)) and RPE tissues (Figs. 3(c), 4(b)–(d), 5(g)). However, the integration of iRPESCs into the retina (Figs. 3(b) and 5(f)) is still doubtful, as possible fusion of transplanted cells to the host cells has been proven to be the most common case in subretinal transplantation [35,36]. Therefore, we were not certain whether the visual retention of the affected retinas damaged by $NaIO_3$ was due to the replacement of the damaged photoreceptors, fusion with the bordering photoreceptors, or simply paracrine effects of the transplanted cells (or a combination thereof). However, we did notice that the number of transplanted iRPESCs continuously decreased over time in the retina and RPE tissues, except for the large clump in the subretinal space. The cause of the disappearance of the iRPESCs was not investigated, but it was likely due to death resulting from immune rejection by host tissues and/or a lack of nutrients and/or oxygen in the subretinal space. Therefore, to perform a long-term study of grafted iRPESC functionality *in vivo*, an immunodeficient mouse model is needed for cell transplantation [33,34].

4.4. RPE spheres and ESC-derived retinal organoids

It is amazing that mouse ESCs can form aggregates in suspension culture that eventually become highly organized retinal organoids in 2–3 weeks [47−49]. These artificial immature retinal tissues could be transplanted into the subretinal space after careful dissection to achieve a corrected orientation; visual recovery was detected after the integration and functioning of the grafted artificial tissues in the host tissues [50]. The authors indicated that transplantation of immature retinal progenitors is critical for the cells to be able to integrate and connect to host neurons [50]. We found that iRPESCs were of dual potential and did not need to be differentiated before transplantation; however, whether they were the progenitors of all detected retinal neurons was not clear.

Declaration of competing interest

The authors declare no competing financial interests.

Acknowledgements

We thank our colleagues Dr. Qingxian Lu for the gift of the mouse fibroblast cell line SNL and Guirong Liu for her assistance in tissue cryosectioning.

Funding sources

This work was supported by the National Natural Science Foundation of China (3087282 and 81072221 to L.G., 81271034 to X.P.) and the Natural Science Foundation of Hunan Province (14JJ2005 to L.G.), National Institute of Health (EY024110 to D.C.D., P20GM103453 to Y. L.), Basic Research Grant of University of Louisville School of Medicine (E0819 to Y.L.), and Research to Prevent Blindness (to DOVS). The funders had no role in study design, data collection, data analysis, interpretation, writing of the report.

Authors' Contributions

F.C., X.L., and Y.C.: performed most of the experiments, collected and analyzed the data, wrote the manuscript; J.Y.L.: conducted the cell differentiation experiment for the final revision; H.L., W.W.: assisted in subretinal injection; X.L.: assisted in RNA extraction and Western blot analysis; K.C.D.: real-time quantitative PCR analyses; L. G. and H.J.K.: designing the experiments and analyzing the data; D.C. D, X.P. and Y.L.: designed experiments, analyzed the data, and wrote the manuscript. All authors read and approved the final manuscript.

Supplementary materials

Supplementary material associated with this article can be found in the online version at doi:10.1016/j.ebiom.2019.102618.

References

[1] Nagase H, Ghosh S. Epigenetics: differential DNA methylation in mammalian somatic tissues. FEBS J 2008;275(8):1617–23.
[2] Goichberg P. Current understanding of the pathways involved in adult stem and progenitor cell migration for tissue homeostasis and repair. Stem Cell Rev 2016;12(4):421–37.
[3] Huang Y, Enzmann V, Ildstad ST. Stem cell-based therapeutic applications in retinal degenerative diseases. Stem Cell Rev 2011;7(2):434–45.

[4] Li T, Lewallen M, Chen S, Yu W, Zhang N, Xie T. Multipotent stem cells isolated from the adult mouse retina are capable of producing functional photoreceptor cells. Cell Res 2013;23(6):788–802.
[5] Fischer AJ, Reh TA. Potential of Muller glia to become neurogenic retinal progenitor cells. Glia 2003;43(1):70–6.
[6] Salero E, Blenkinsop TA, Corneo B, Harris A, Rabin D, Stern JH, et al. Adult human RPE can be activated into a multipotent stem cell that produces mesenchymal derivatives. Cell Stem Cell 2012;10(1):88–95.
[7] Chichagova V, Hallam D, Collin J, Zerti D, Dorgau B, Felemban M, et al. Cellular regeneration strategies for macular degeneration: past, present and future. Eye (Lond) 2018;32(5):946–71.
[8] Lamba DA, Gust J, Reh TA. Transplantation of human embryonic stem cell-derived photoreceptors restores some visual function in Crx-deficient mice. Cell Stem Cell 2009;4(1):73–9.
[9] Tang Z, Zhang Y, Wang Y, Zhang D, Shen B, Luo M, et al. Progress of stem/progenitor cell-based therapy for retinal degeneration. J Transl Med 2017;15(1):99.
[10] Stanzel BV, Liu Z, Somboonthanakij S, Wongsawad W, Brinken R, Eter N, et al. Human RPE stem cells grown into polarized RPE monolayers on a polyester matrix are maintained after grafting into rabbit subretinal space. Stem Cell Rep 2014;2(1):64–77.
[11] Haynes T, Del Rio-Tsonis K. Retina repair, stem cells and beyond. Curr Neurovasc Res 2004;1(3):231–9.
[12] Yang S, Li H, Li M, Wang F. Mechanisms of epithelial-mesenchymal transition in proliferative vitreoretinopathy. Discov Med 2015;20(110):207–17.
[13] Liu Y, Mukhopadhyay P, Pisano MM, Lu X, Huang L, Lu Q, et al. Repression of Zeb1 and hypoxia cause sequential mesenchymal-to-epithelial transition and induction of aid, Oct4, and Dnmt1, leading to immortalization and multipotential reprogramming of fibroblasts in spheres. Stem Cells 2013;31(7):1350–62.
[14] Franco LM, Zulliger R, Wolf-Schnurrbusch UE, Katagiri Y, Kaplan HJ, Wolf S, et al. Decreased visual function after patchy loss of retinal pigment epithelium induced by low-dose sodium iodate. Investig Ophthalmol Vis Sci 2009;50(8):4004–10.
[15] Enzmann V, Row BW, Yamauchi Y, Kheirandish L, Gozal D, Kaplan HJ, et al. Behavioral and anatomical abnormalities in a sodium iodate-induced model of retinal pigment epithelium degeneration. Exp Eye Res 2006;82(3):441–8.
[16] Pan C, Hicks A, Guan X, Chen H, Bishop CE. SNL fibroblast feeder layers support derivation and maintenance of human induced pluripotent stem cells. J Genet Genomics 2010;37(4):241–8.
[17] Liu Y, Ye F, Li Q, Tamiya S, Darling DS, Kaplan HJ, et al. Zeb1 represses Mitf and regulates pigment synthesis, cell proliferation, and epithelial morphology. Invest Ophthalmol Vis Sci 2009;50(11):5080–8.
[18] Liu Y, Clem B, Zuba-Surma EK, El-Naggar S, Telang S, Jenson AB, et al. Mouse fibroblasts lacking RB1 function form spheres and undergo reprogramming to a cancer stem cell phenotype. Cell Stem Cell 2009;4(4):336–47.
[19] Wang W, Noel J, Kaplan HJ, Dean DC. Circulating reactive oxidant causes apoptosis of retinal pigment epithelium and cone photoreceptors in the mouse central retina. Ophthalmol Eye Dis 2011;3:45–54.
[20] Livak KJ, Schmittgen TD. Analysis of relative gene expression data using real-time quantitative PCR and the 2(-Delta Delta C(T)) Method. Methods 2001;25(4):402–8.
[21] Lei QY, Zhang H, Zhao B, Zha ZY, Bai F, Pei XH, et al. TAZ promotes cell proliferation and epithelial-mesenchymal transition and is inhibited by the hippo pathway. Mol Cell Biol 2008;28(7):2426–36.
[22] Liu Y, El-Naggar S, Darling DS, Higashi Y, Dean DC. Zeb1 links epithelial-mesenchymal transition and cellular senescence. Development 2008;135(3):579–88.
[23] Reh TA, Levine EM. Multipotential stem cells and progenitors in the vertebrate retina. J Neurobiol 1998;36(2):206–20.
[24] Hiscott P, Sheridan C, Magee RM, Grierson I. Matrix and the retinal pigment epithelium in proliferative retinal disease. Prog Retin Eye Res 1999;18(2):167–90.
[25] Reh TA, Fischer AJ. Retinal stem cells. Methods Enzymol 2006;419:52–73.
[26] Osakada F, Ikeda H, Sasai Y, Takahashi M. Stepwise differentiation of pluripotent stem cells into retinal cells. Nat Protoc 2009;4(6):811–24.
[27] Kleemann M, Schneider H, Unger K, Sander P, Schneider EM, Fischer-Posovszky P, et al. MiR-744-5p inducing cell death by directly targeting HNRNPC and NFIX in ovarian cancer cells. Sci Rep 2018;8(1):9020.
[28] Xu N, Chen Y, Dean KC, Lu X, Liu X, Wang W, et al. Sphere-induced rejuvenation of swine and human muller glia is primarily caused by telomere elongation. Stem Cells 2017;35(6):1579–91.
[29] Cheng T. Cell cycle inhibitors in normal and tumor stem cells. Oncogene 2004;23(43):7256–66.
[30] Takahashi K, Yamanaka S. Induction of pluripotent stem cells from mouse embryonic and adult fibroblast cultures by defined factors. Cell 2006;126(4):663–76.
[31] Field JK, Spandidos DA. The role of ras and myc oncogenes in human solid tumours and their relevance in diagnosis and prognosis (review). Anticancer Res 1990;10(1):1–22.
[32] Geraerts M, Verfaillie CM. Adult stem and progenitor cells. Adv Biochem Eng Biotechnol 2009;114:1–21.
[33] Iraha S, Tu HY, Yamasaki S, Kagawa T, Goto M, Takahashi R, et al. Establishment of immunodeficient retinal degeneration model mice and functional maturation of human ESC-derived retinal sheets after transplantation. Stem Cell Reports 2018;10(3):1059–74.
[34] Mishra A, Das B, Nath M, Iyer S, Kesarwani A, Bhattacharjee J, et al. A novel immunodeficient NOD.SCID-rd1 mouse model of retinitis pigmentosa to investigate potential therapeutics and pathogenesis of retinal degeneration. Biol Open 2017;6(4):449–62.
[35] Singh MS, Balmer J, Barnard AR, Aslam SA, Moralli D, Green CM, et al. Transplanted photoreceptor precursors transfer proteins to host photoreceptors by a mechanism of cytoplasmic fusion. Nat Commun 2016;7:13537.
[36] Pearson RA, Gonzalez-Cordero A, West EL, Ribeiro JR, Aghaizu N, Goh D, et al. Donor and host photoreceptors engage in material transfer following transplantation of post-mitotic photoreceptor precursors. Nat Commun 2016;7:13029.
[37] Heneidi S, Simerman AA, Keller E, Singh P, Li X, Dumesic DA, et al. Awakened by cellular stress: isolation and characterization of a novel population of pluripotent stem cells derived from human adipose tissue. PLoS One 2013;8(6):e64752.
[38] Yamasaki S, Anderson P. Reprogramming mRNA translation during stress. Curr Opin Cell Biol 2008;20(2):222–6.
[39] Jacque E, Schweighoffer E, Tybulewicz VL, Ley SC. BAFF activation of the ERK5 MAP kinase pathway regulates B cell survival. J Exp Med 2015;212(6):883–92.
[40] Hornyak TJ, Jiang S, Guzman EA, Scissors BN, Tuchinda C, He H, et al. Mitf dosage as a primary determinant of melanocyte survival after ultraviolet irradiation. Pigment Cell Melanoma Res 2009;22(3):307–18.
[41] Pieters T, van Roy F. Role of cell-cell adhesion complexes in embryonic stem cell biology. J Cell Sci 2014;127(Pt 12):2603–13.
[42] Zhao B, Tumaneng K, Guan KL. The Hippo pathway in organ size control, tissue regeneration and stem cell self-renewal. Nat Cell Biol 2011;13(8):877–83.
[43] Larsen JE, Nathan V, Osborne JK, Farrow RK, Deb D, Sullivan JP, et al. ZEB1 drives epithelial-to-mesenchymal transition in lung cancer. J Clin Invest 2016;126(9):3219–35.
[44] Liu Y, Xin Y, Ye F, Wang W, Lu Q, Kaplan HJ, et al. Taz-tead1 links cell-cell contact to zeb1 expression, proliferation, and dedifferentiation in retinal pigment epithelial cells. Invest Ophthalmol Vis Sci 2010;51(7):3372–8.
[45] Park JH, Shin JE, Park HW. The role of hippo pathway in cancer stem cell biology. Mol Cells 2018;41(2):83–92.
[46] Harvey DM, Levine AJ. p53 alteration is a common event in the spontaneous immortalization of primary BALB/c murine embryo fibroblasts. Genes Dev 1991;5(12B):2375–85.
[47] DiStefano T, Chen HY, Panebianco C, Kaya KD, Brooks MJ, Gieser L, et al. Accelerated and improved differentiation of retinal organoids from pluripotent stem cells in rotating-wall vessel bioreactors. Stem Cell Rep 2018;10(1):300–13.
[48] Chen HY, Kaya KD, Dong L, Swaroop A. Three-dimensional retinal organoids from mouse pluripotent stem cells mimic in vivo development with enhanced stratification and rod photoreceptor differentiation. Mol Vis 2016;22:1077–94.
[49] Volkner M, Zschatzsch M, Rostovskaya M, Overall RW, Busskamp V, Anastassiadis K, et al. Retinal organoids from pluripotent stem cells efficiently recapitulate retinogenesis. Stem Cell Reports 2016;6(4):525–38.
[50] McLelland BT, Lin B, Mathur A, Aramant RB, Thomas BB, Nistor G, et al. Transplanted hESC-derived retina organoid sheets differentiate, integrate, and improve visual function in retinal degenerate rats. Investig Ophthalmol Vis Sci 2018;59(6):2586–603.